PAPER

Strategic integration of nitroimino and dinitromethyl explophores onto tetrazole: K$_2$DNMNAT as a material with enhanced thermal stability and optimized oxygen balance†

Parul Saini,[a] Jatinder Singh, [ID][a] Richard J. Staples [ID][b] and Jean'ne M. Shreeve [ID] *[a]

Enhancing the energy output of tetrazole-based materials through nitro functionalization often compromises thermal stability, posing a significant challenge in developing advanced energetic materials. In this study, we address this issue by strategically integrating both nitroimino and dinitromethyl high-energy functional groups onto the tetrazole ring, along with the incorporation of two potassium ions, yielding dipotassium 4-(dinitromethaneidyl)-5-(nitroimino)-4,5-dihydrotetrazol-1-ide (K$_2$DNMNAT). Structural characterization confirmed the successful one-step nitration, while thermal and energetic assessments demonstrated an optimal balance between stability and performance. Comparative analysis with previously reported tetrazole-based nitroimino salts reveals that K$_2$DNMNAT exhibits superior oxygen balance without compromising the decomposition temperature. Furthermore, when evaluated against tetrazole-based dinitromethyl-containing compounds, remarkable thermal resilience and enhanced energetic properties are found. Sensitivity tests indicate that this new nitroimino tetrazole exhibits mechanical stability within established safety thresholds in comparison with potassium-based primary explosives. Combining a straightforward synthesis, potassium-assisted stabilization, improved oxygen balance, and robust thermal stability positions, K$_2$DNMNAT is seen to be a promising contender for next-generation energetic materials with enhanced performance and safety.

Introduction

Tetrazole and its derivatives have garnered significant attention in the field of energetic materials due to their high nitrogen content (80%) and favorable positive heat of formation ($\Delta H_f =$ 4.77 kJ g^{-1}). These characteristics make tetrazole a valuable backbone for high-performance energetic compounds, particularly for applications requiring high energy density, rapid decomposition rates, and environment friendliness.[1-6] However, functionalizing the tetrazole ring remains a formidable challenge due to the limited number of reactive sites available for substitution. Traditionally, modifications have been restricted to the C5 and N1 positions, with some reported functionalization at both positions. Despite these efforts, expanding the tunability of tetrazole-based compounds for enhanced energetic performance while maintaining structural stability remains a crucial objective.[7-28]

Due to the limited functionality of tetrazole, its modification has primarily relied on linear substitutions, incorporating energetic groups such as additional tetrazole rings, azo (–N≡N–) linkages, and methylene (–CH$_2$–) bridges. While these modifications have improved energetic performance in some cases, they often have led to reduced molecular density. Additionally, integrating high-energy groups, such as nitro (–NO$_2$) or dinitromethyl [–C(NO$_2$)$_2$], frequently results in decreased thermal stability, thereby limiting their practical applications. This trade-off between energy and stability poses a major challenge in the design of next-generation environmentally friendly energetic materials. To overcome this limitation, an innovative and facile approach that strategically integrates high-energy functional groups without compromising thermal resilience is essential.
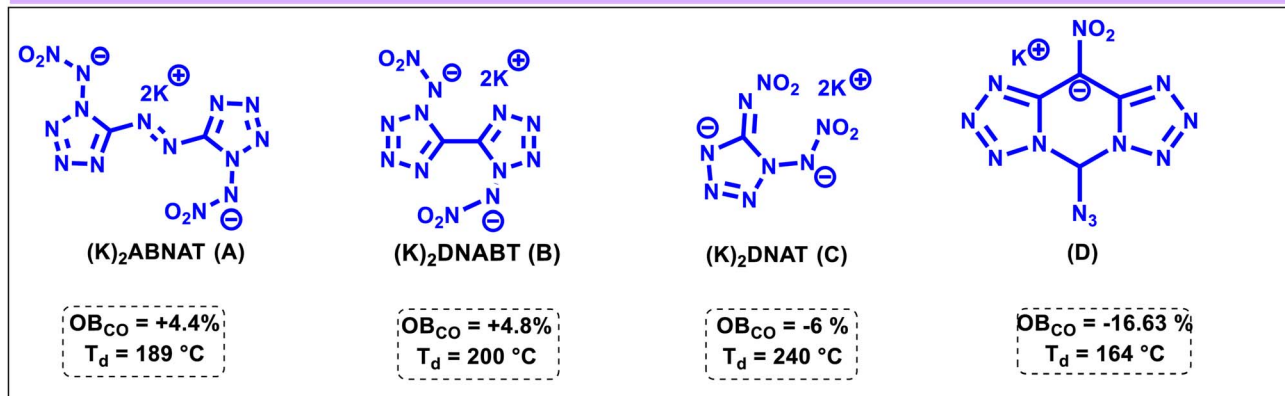
Coordination chemistry principles enable the precise organization of molecules or metal ions into stable, well-defined structures, allowing researchers to fine-tune these arrangements to optimize properties such as sensitivity, thermal stability, and energy output in energetic materials.[29-33] Recent advances have focused on potassium salts with tetrazole backbones, since the tetrazole ring behaves as an environmentally friendly and versatile ligand, forming coordination bonds with various metal ions (Fig. 1A). Compounds such as 5,5′-azobis(1-

[a]Department of Chemistry, University of Idaho, Moscow, ID 83844-2343, USA. E-mail: jshreeve@uidaho.edu

[b]Department of Chemistry, Michigan State University, East Lansing, Michigan 48824, USA

This journal is © The Royal Society of Chemistry 2025
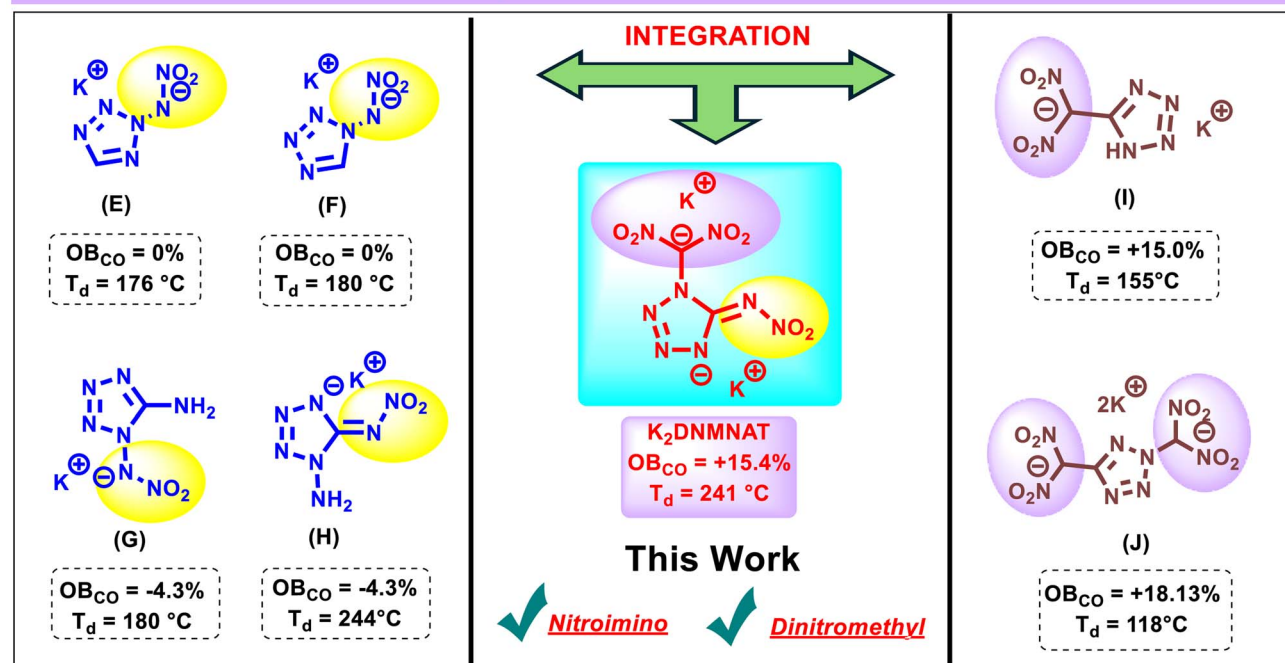
J. Mater. Chem. A, 2025, **13**, 17421–17428 | **17421**

nitroimino tetrazolate) (**K₂ABNAT**), potassium dinitroimino-5,5′-bistetrazolate ((**K**)**₂DNABT**), potassium 4,5-bis(dinitromethyl)furoxannate (**K₂BDNMF**), and compound **D** (potassium 5-azido-10-nitro-bis(tetrazolo)[1,5-*c*:5′,1′-*f*]pyrimidinium) have shown promise as potential replacements for environmentally harmful lead azide-based primary explosives.[34–38]

(**K₂ABNAT**), potassium dinitroimino-5,5′-bistetrazolate ((**K**)**₂DNABT**), potassium 4,5-bis(dinitromethyl)furoxannate (**K₂BDNMF**), and compound **D** (potassium 5-azido-10-nitro-bis(tetrazolo)[1,5-*c*:5′,1′-*f*]pyrimidinium) have shown promise as potential replacements for environmentally harmful lead azide-based primary explosives.[34–38]
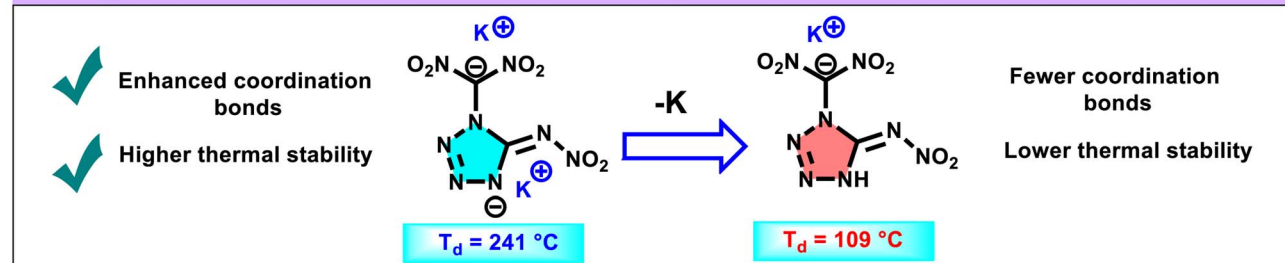

Fig. 1 A comparative study of tetrazole moiety-based potassium salts was previously reported, and this work. (A) Some previously reported green primary explosives. (B) Potassium salts based on a tetrazole ring. (C) Comparison of mono- and dipotassium salts of this study.

17422 | *J. Mater. Chem. A*, 2025, **13**, 17421–17428

This journal is © The Royal Society of Chemistry 2025

Further investigations into potassium-substituted tetrazole compounds have revealed important insights into their thermal stability and oxygen balance. Potassium salts featuring a single nitroimino functionalization, such as compounds **E** (potassium 2-(N-nitramino)-5H-tetrazolate) and **F** (potassium 1-(N-nitramino)-5H-tetrazolate), exhibit decomposition temperatures of 176 °C and 180 °C, respectively, with an oxygen balance (OB) of 0% (Fig. 1B). However, attempts to enhance thermal resilience by introducing an amino (–NH₂) group vicinal to nitroimino functionalities, as observed in compounds **G** (potassium 1-nitrimino-5-aminotetrazolate) and **H** (potassium 1-amino-5-nitriminotetrazolate), resulted in a decreased OB of −4.3%, further emphasizing the challenge of optimizing both stability and energetic output. Efforts to improve oxygen balance through the incorporation of dinitromethyl (–C(NO₂)₂) groups, as seen in compounds **I** (potassium 5-(dinitromethyl)-1H-tetrazolate) and **J** (dipotassium (2H-tetrazole-2,5-diyl)bis(dinitromethanide), failed to maintain adequate thermal stability, illustrating the inherent difficulty in achieving a synergy between oxygen balance and decomposition temperature. While increasing the number of nitro groups generally enhances oxygen balance, density, and detonation parameters—factors crucial for applications in rocket propulsion and high-performance explosives—the corresponding reduction in thermal stability remains a significant drawback. These findings underscore the pressing need for a rational functionalization strategy that maximizes both energy and structural integrity.[39–43]

In this study, tetrazole was functionalized strategically by the successful incorporation of both nitroimino and dinitromethyl functional groups onto the tetrazole ring, while simultaneously introducing potassium metal to enhance structural stability. The incorporation of potassium ions facilitated the formation of new coordination bonds, thereby contributing to the overall stability of the compound. This innovative strategy resulted in the synthesis of dipotassium 4-(dinitromethaneidyl)-5-(nitroimino)-4,5-dihydrotetrazol-1-ide (**K₂DNMNAT**), which exhibits a remarkable balance of thermal stability and oxygen balance, addressing the limitations encountered in previous derivatives effectively.
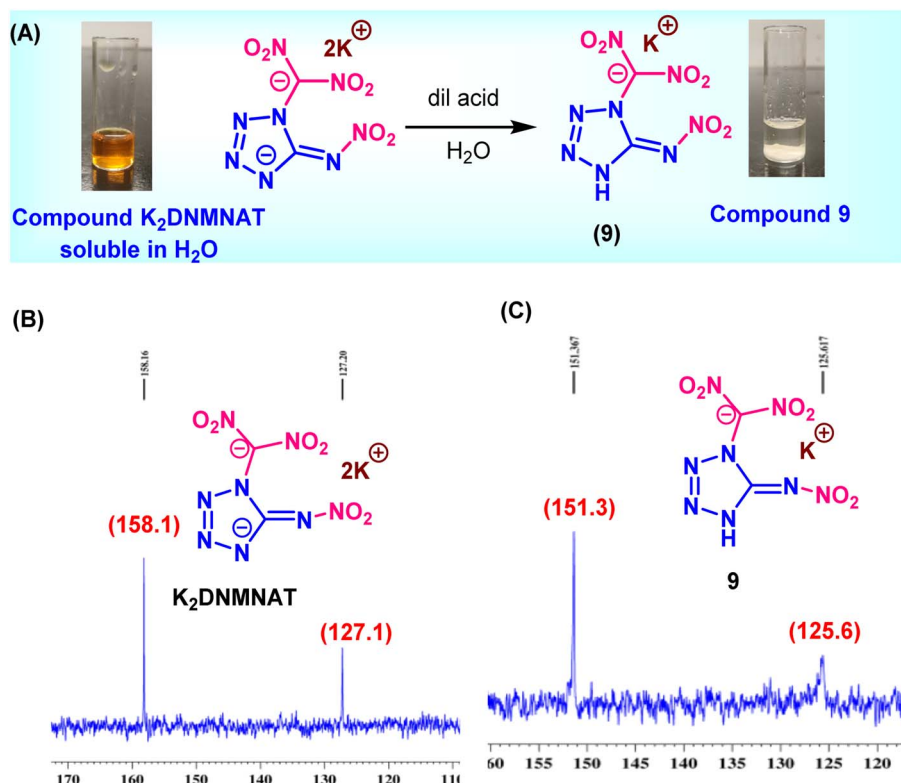
Results and discussion

To synthesize **K₂DNMNAT**, two strategies are considered. The first strategy involves the isolation of the sensitive nitramine compound **4** (Scheme 1). This route consists of four steps, including two nitration steps. In contrast, the second strategy begins with the facile synthesis of stable derivative **2**. Upon the reaction of compound **2** with mixed acid (HNO₃/H₂SO₄), double nitration occurs, resulting in the formation of compound **3**. The crude mixture is treated directly with NH₂OH·HCl/KOH to yield **K₂DNMNAT** in quantitative yield.[44,45]
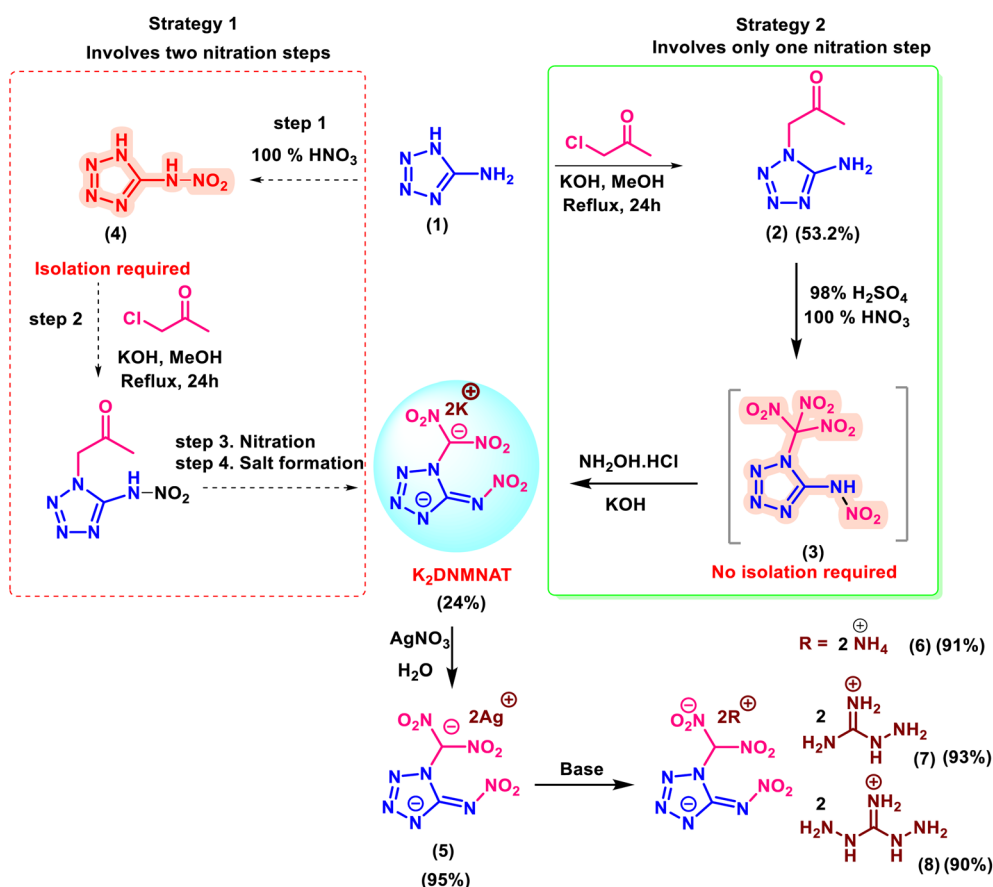
Scheme 1 Synthesis of dipotassium-4-(dinitromethaneidyl)-5-(nitroimino)-4,5-dihydrotetrazol-1-ide (**K₂DNMNAT**) and its salts (**5–8**).

This journal is © The Royal Society of Chemistry 2025

J. Mater. Chem. A, 2025, **13**, 17421–17428 | **17423**

Scheme 2 (A) Synthesis of potassium dinitro(5-(nitroimino)-4,5-dihydro-1H-tetrazol-1-yl) methanide (**9**). (B) ^{13}C NMR of compound **K₂-DNMNAT**, (C) ^{13}C NMR of compound **9**.

K₂DNMNAT is reacted with AgNO₃ to make the corresponding silver salt (**5**). The subsequent treatment of **5** with NH₄Cl gives the ammonium salt (**6**). The energetic salts **7** and **8** were synthesized by reacting compound **K₂DNMNAT** with aminoguanidine·HCl and diamminoguanidine·HCl, respectively. It is observed that neutralization of **K₂DNMNAT** with dilute acid to make a neutral derivative resulted in the selective isolation of the mono potassium salt **9**. Interestingly, compound **9** precipitates due to strong intramolecular hydrogen bonding (Scheme 2A).

The characterization of compounds **K₂DNMNAT** and **9** was performed using NMR spectroscopy. In the ^{13}C NMR spectrum of compound **K₂DNMNAT**, two distinct peaks were seen at 158.1 ppm (tetrazole carbon) and 127.1 ppm (dinitromethyl group carbon). In contrast, for compound **9**, the tetrazole carbon peak is shifted to 151 ppm, while the dinitromethyl group carbon peak exhibited only a slight change to 125.6 (Schemes 2B and C). These results suggest that neutralization first occurs at the nitramine functional group rather than the dinitromethylene carbon.

Single-crystal X-ray crystallography

Attempts to obtain high-quality single crystals of compound **K₂DNMNAT** suitable for X-ray diffraction were conducted using various organic solvents. However, the crystalline nature of the compound was lost upon solvent evaporation. Crystallization from DMSO yielded suitable single crystals with two molecules
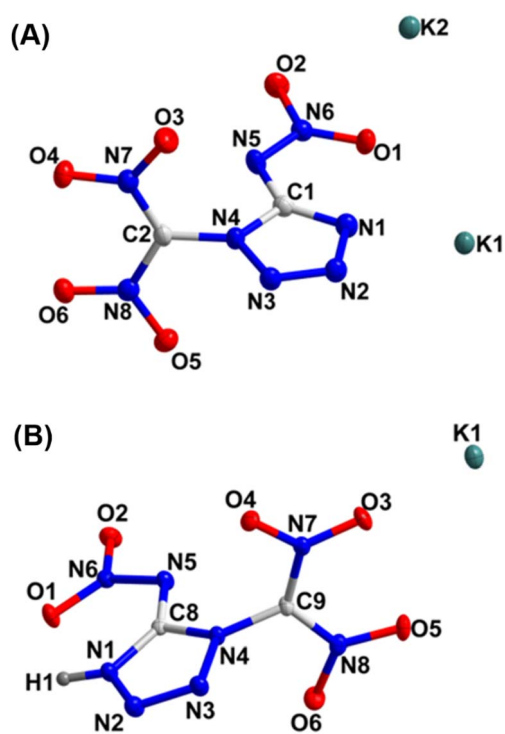

Fig. 2 (A) Drawing at 50% ellipsoids of compound **K₂-DNMNAT·2DMSO**. (B) Drawing at 50% ellipsoids of compound **9·H₂O**. (DMSO and H₂O are omitted for clarity).

17424 | *J. Mater. Chem. A*, 2025, **13**, 17421–17428

This journal is © The Royal Society of Chemistry 2025

of DMSO. Compound **K₂DNMNAT·2DMSO** crystallizes in the monoclinic space group $P2_1/c$ with a calculated density of 1.785 g cm⁻³ at 101 K. As illustrated in Fig. 2A, the tetrazole ring and the nitroimino group are nearly coplanar, whereas the dinitromethyl group is oriented in a different plane.

Compound **9·H₂O** crystallizes in the monoclinic space group $C2/c$ with a crystal density of 2.025 g cm⁻³ at 100 K (Fig. 2B). As depicted in Fig. 2A, similar to the crystal structure of compound **K₂DNMNAT·2DMSO**, the tetrazole and nitroimino groups in compound **9·H₂O** are nearly coplanar, while the nitromethyl group is positioned in a different plane. Hydrogen bonding interactions are observed with a maximum donor–acceptor (D⋯D) distance of 3.11 Å and a minimum bond angle of 110°. The specific hydrogen bonding interactions include O1W–O2_1: 3.006 Å, O1W–O4_2: 2.866 Å, O1W–O6_3: 2.728 Å, and N1–O1W_4: 2.626 Å.

Physicochemical and detonation properties

The thermal behavior of compounds **K₂DNMNAT**, **6**, **7·H₂O**, **8·2H₂O**, and **9·H₂O** was analyzed using differential scanning calorimetry (DSC) at a heating rate of 5 °C min⁻¹ under an N₂ atmosphere (Table 1). Among these, the dipotassium salt (**K₂-DNMNAT**) exhibited the highest decomposition temperature at 241 °C. The decomposition temperatures of compounds **6**,
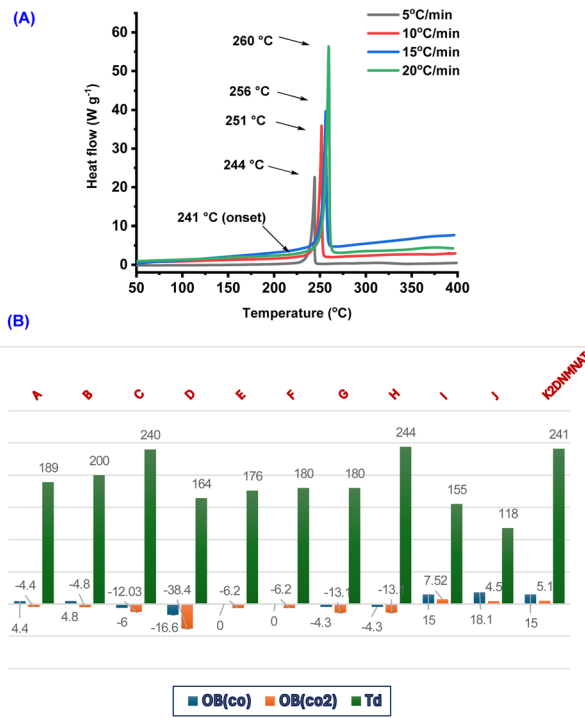

Fig. 3 (A) DSC plots of K₂DNMNAT at different heating rates. (B) Comparison graph of oxygen balance and thermal stability for A–J and K2DNMNAT.

Table 1 Physicochemical properties of compounds K2DNMNAT, 6, 7·H₂O, 8·2H₂O and 9·H₂O and comparison with traditional primary explosive

Comp.	$T_d{}^a$ (°C)	OB$_{CO/CO2}$ (%)	ρ^b (g cm⁻³)	$\Delta H_f{}^c$ (kJ mol⁻¹)	P^d (GPa)	$D_v{}^e$ (m s⁻¹)	IS^f (J)	FS^g (N)
K₂DNMNAT	241	+15.4/+5.1	2.08	−106.7	24.6	7661	1	10
6	145	0/−11.9	1.75	157.9	33.2	8985	1	20
7·H₂O	137	−19.9/−35.9	1.65	199.6	26.5	8471	1	40
8·2H₂O	119	−21.4/−35.6	1.68	186.9	29.0	8835	2	40
9·H₂O	107	+16.5/+5.5	1.96^h	−6.4	30.2	8447	3	20
LA^i	315	−11/−11	4.08	450.1	33.8	5920	2.5–4	1
LS^j	282	−5.7/−8.0	3.06	−835	—	5200	2.5–5	1.5
KDNP^k	260	0/−34.2	1.95	−461.7	20.01	6952	0.05	9.8
DTAT-K^l	163.6	−19.4/−38.4	1.88	326.4	31.7	7917	1	20
(K)₂DNABT^m	200	4.8/−4.8	2.11	970.97	25.2	8330	5	<1

^{a} Temperature (onset) of decomposition. ^{b} Density at 25 °C using gas pycnometer. ^{c} Molar enthalpy of formation, calculated using isodesmic reactions with the Gaussian 03 suite of programs (revision D.01). ^{d} Detonation pressure. ^{e} Detonation velocity (calculated using EXPLO5 version 7.01.01). ^{f} Sensitivity to impact (IS). ^{g} Sensitivity to friction (FS). ^{h} X-ray density calculated at room temperature (RT). ^{i} ref. 49. ^{j} ref. 50. ^{k} ref. 51. ^{l} ref. 32. ^{m} ref. 28.

$7 \cdot H_2O$, $8 \cdot 2H_2O$, and $9 \cdot H_2O$ are 145, 137, 119, and 107 °C, respectively.

Based upon peak decomposition temperatures measured by differential scanning calorimetry (DSC) for compound K_2-**DNMNAT** at different heating rates of 5, 10, 15, and 20 °C min^{-1} (Fig. 3A), the activation energies (E_k and E_0), and linear correlation coefficients (R_k and R_0) were calculated using Kissinger's[46] and Ozawa's[47] methods and are given in Tables S5 and S6 (ESI).† The results show that the activation energy calculated by either method is essentially the same ($E_k = 190.4$ kJ mol^{-1}; $E_0 = 189.3$ kJ mol^{-1}). Depending upon the calculated numerical values of E_k, the rate constant of decomposition can be expressed as $\ln k = \ln A_k - (190.4 \times 10^3)/RT$. The low activation energy of K_2**DNMNAT**, which falls in the range of reported

primary explosives, indicates that it can be easily stimulated for intense chemical reactions.[48]

The comparative study of oxygen balance and thermal stability of K_2**DNMNAT** with previously reported potassium salts is presented in Fig. 3B. This study demonstrates that K_2-**DNMNAT** exhibits an optimal balance between energy and safety compared to the previously reported compounds (**A–J**). The Hirshfeld surface analyses for K_2**DNMNAT** and **9** were performed and are shown in Fig. 4A and B.

On the edges of the Hirshfeld surface of K_2**DNMNAT** and **9**, many red regions (high close-contact population) were observed, which are mainly due to coordination bonds, i.e., K···O contacts, and contribute 26.7% and 20.3% for K_2**DNMNAT** and **9**, respectively to the total interactions (Fig. 3C

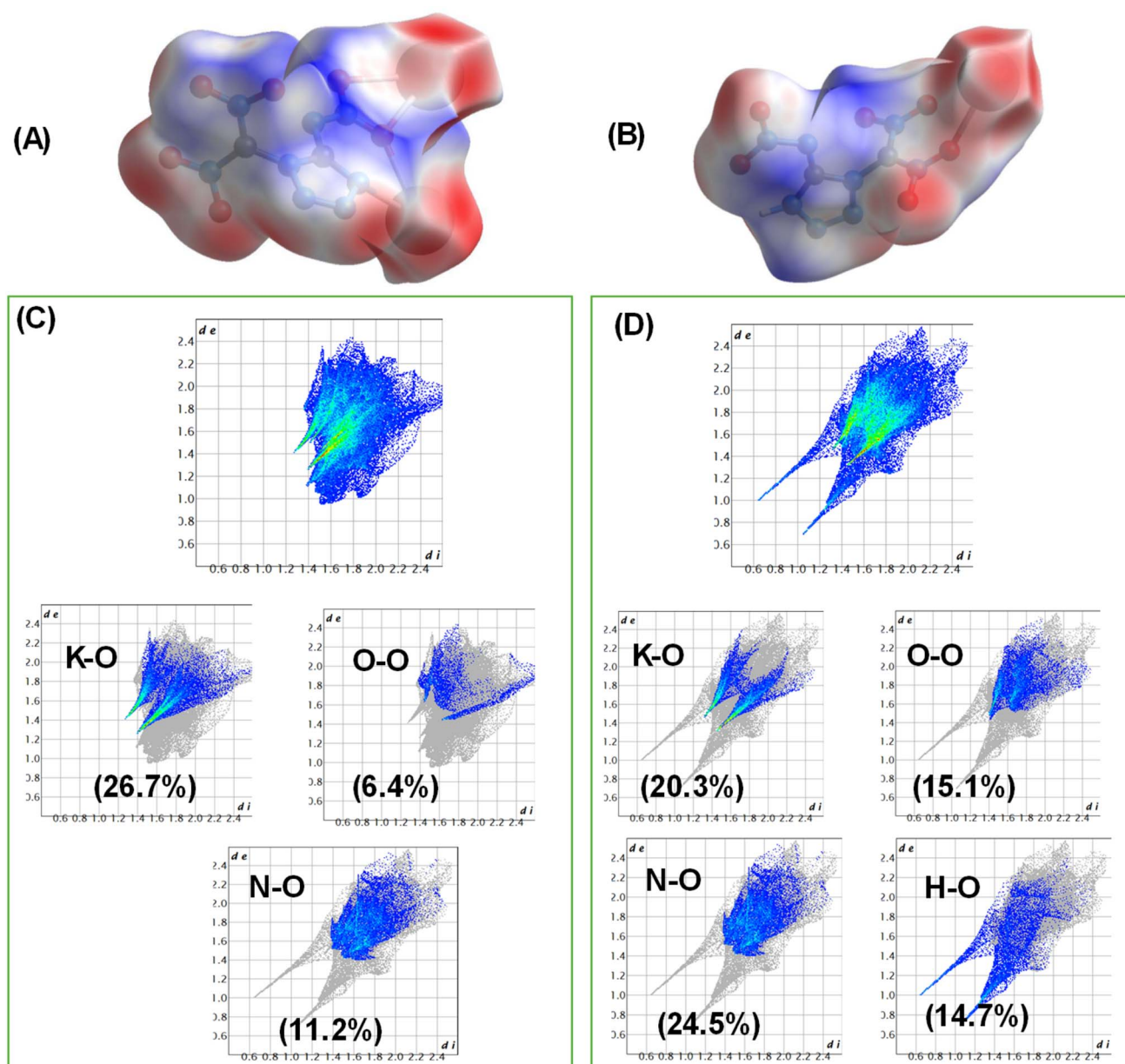Fig. 4 (A and B) Hirshfeld surfaces for K_2DNMNAT and 9 (C and D) 2D fingerprint plots for compound K_2DNMNAT and 9.

17426 | J. Mater. Chem. A, 2025, 13, 17421–17428

This journal is © The Royal Society of Chemistry 2025

A. Hot needle test

B. Hot plate test

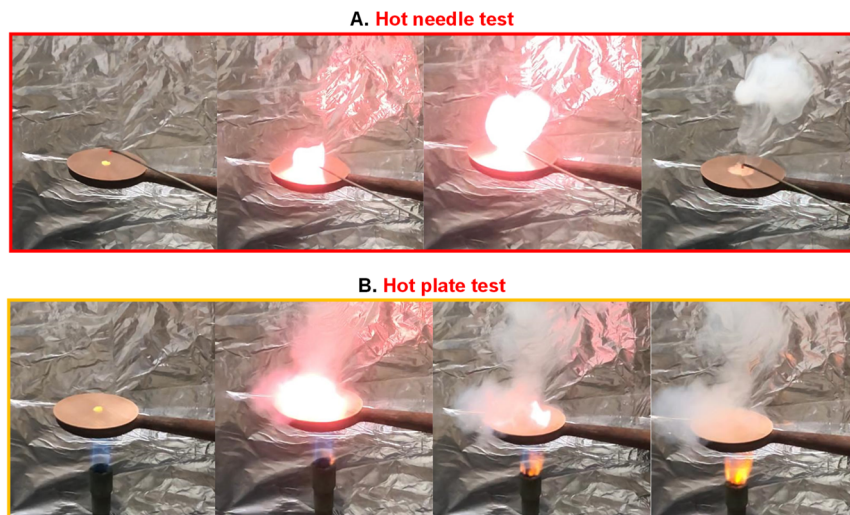**Fig. 5** (A) Hot needle test for K2DNMNAT. (B) Hot plate test for K2DNMNAT.

and D). The larger value of K⋯O contacts stabilizing interactions enhances molecular stability. The impact and friction sensitivities of compounds **K₂DNMNAT**, **6**, **7·H₂O**, **8·2H₂O**, and **9·H₂O** were assessed using BAM standard methods, and the results are summarized in Table 1. All compounds demonstrated sensitivity to mechanical stimuli. The experimental densities of the compounds were measured using a gas pycnometer at a controlled temperature of 25 °C. Notably, compound **K₂DNMNAT** exhibited better friction sensitivity (FS) than **LA**, **LS**, **KDNP**, and **(K)₂DNABT**. **K₂DNMNAT** also showed an oxygen balance (OB) of +15.5%, which is significantly higher than that of **LA**, **LS**, **KDNP**, **DTAT-K**, and **(K)2DNABT**, making it more environmentally favorable compared to these previously reported compounds. The experimental densities and calculated enthalpies of formation were further utilized in the EXPLO5 (v7.01.01) software to predict the detonation properties of these compounds. The results indicated that compound **6** exhibited the highest calculated detonation velocity of 8985 m s⁻¹. **K₂DNMNAT**'s detonation velocity surpassed that of **LA**, **LS**, and **KDNP**, suggesting enhanced explosive characteristics. Its detonation velocity is also comparable to that of **DTAT-K**.

LA, **LS**, and **KDNP** demonstrate good thermal stability. They have lower oxygen balances and detonation velocities compared to **K₂DNMNAT**. On the other hand, **DTAT-K** and **(K)₂DNABT** exhibit better detonation velocities but have lower thermal stability and oxygen balance.

Experiments such as the "red-hot needle" and "heated plate" tests were conducted on a 10 mg sample of K₂DNMNAT to evaluate its energetic behavior (Fig. 5A and B). The red-hot needle test revealed a sharp deflagration accompanied by a visible flame, as shown in Fig. 5A. Similarly, the heated plate test also demonstrated deflagration, confirming the energetic nature of the compound.

In conclusion, the synthesis of dipotassium 4-(dinitromethaneidyl)-5-(nitroimino)-4,5-dihydrotetrazol-1-ide (**K₂DNMNAT**) illustrates a significant advance in the development of potassium metal-based energetic salts. The careful tuning of nitro groups has proven crucial in achieving a desirable equilibrium between energy output and stability, a challenge that continues to define the landscape of energetic materials. We have synthesized the **6**, **7**, and **9** energetic salts, which also show good energy properties. Furthermore, their compatibility with other energetic materials enhances their potential as promising candidates for new high-energy-density materials with practical applications.

Data availability

All data relevant to the work described here are available in the ESI.†

Conflicts of interest

There are no conflicts to declare.

Acknowledgements

References

1 J. Zhou, J. Zhang, B. Wang, L. Qiu, R. Xu and A. B. Sheremetev, *FirePhysChem*, 2024, **2**, 83–139.

2 J. Cai, T. Fei, R. Li, J. Xiong, J. Zhang, P. Yin and S. Pang, *ACS Appl. Mater. Interfaces*, 2022, **14**, 52951–52959.

3 T. M. Klapötke, *Chemistry of High-Energy Materials*, Walter de Gruyter & Co, KG, Berlin-New York, 2012, 2nd edn.

4 T. M. Klapötke, D. G. Piercey, N. Mehta, K. D. Oyler, M. Jorgensen, S. Lenahan, J. S. Salan, J. W. Fronabarger and M. D. Williams, *Anorg. Allg. Chem.*, 2013, **639**, 681–688.

This journal is © The Royal Society of Chemistry 2025

J. Mater. Chem. A, 2025, **13**, 17421–17428 | **17427**

5   C. L. He and J. M. Shreeve, *Angew. Chem., Int. Ed.*, 2016, **55**, 772–775.

6   M. H. V. Huynh, M. A. Hiskey, T. J. Meyer and M. Wetzler, *Proc. Natl. Acad. Sci. U. S. A.*, 2006, **103**, 5409–5412.

7   M. Krawiec, S. R. Anderson, P. Dubé, D. D. Ford, J. S. Salan, S. Lenahan, N. Mehta and C. R. Hamilton, *Propellants, Explos., Pyrotech.*, 2015, **40**, 457–459.

8   L. Zhai, X. Fan, B. Wang, F. Bi, Y. Li and Y. Zhu, *RSC Adv.*, 2015, **5**, 57833–57841.

9   J. A. Garrison and R. M. Herbst, *J. Org. Chem.*, 1957, **22**, 278–283.

10 X. Yu, J. Tang, C. Lei, C. Xue, G. Cheng, C. Xiao and H. Yang, *J. Mater. Chem. A*, 2024, **12**, 19513–19520.

11 X. Yu, J. Tang, C. Lei, C. Xue, H. Yang, C. Xiao and G. Cheng, *J. Mater. Chem. A*, 2024, **12**, 29638–29644.

12 J. Liu, Y. Dong, M. Li, Y. Liu, W. Huang, C. Xiao, G. Cheng and Y. Tang, *J. Org. Chem.*, 2025, **90**(11), 4054–4061.

13 B. Wang, X. Qi, W. Zhang, K. Wang, W. Lia and Q. Zhang, *J. Mater. Chem. A*, 2017, **5**, 20867–20873.

14 J. E. Zuckerman, M. C. St Myer, M. Zeller and D. G. Piercey, *ChemPlusChem*, 2025, **90**, e202400164.

15 J. Singh, R. J. Staples and J. M. Shreeve, *J. Mater. Chem. A*, 2023, **11**, 12896–12901.

16 Y. Yang, W. Zhang, S. Pang, H. Huang and C. Sun, *J. Org. Chem.*, 2024, **89**, 12790–12794.

17 F. Meng, R. Zhou, Z. Xu, P. Wang, Y. Xu and M. Lu, *J. Org. Chem.*, 2025, **90**, 3964–3973.

18 A. F. Tarchoun, D. Trache, T. M. Klapötke and K. Khimeche, *Chem. Eng. J.*, 2020, **400**, 125960.

19 N. Fischer, D. Fischer, T. M. Klapötke, D. G. Piercey and J. Stierstorfer, *J. Mater. Chem.*, 2012, **22**, 20418–20422.

20 N. Fischer, D. Izsák, T. M. Klapötke, S. Rappengluck and J. Stierstorfer, *Chem. - Eur. J.*, 2012, **18**, 4051–4062.

21 N. Fischer, L. Gao, T. M. Klapötke and J. Stierstorfer, *Polyhedron*, 2013, **51**, 201–210.

22 N. Fischer, T. M. Klapötke, M. Reymann and J. Stierstorfer, *Eur. J. Inorg. Chem.*, 2013, **2013**, 2167–2180.

23 K. Hafner, T. M. Klapötke, P. C. Schmid and J. Stierstorfer, *Eur. J. Inorg. Chem.*, 2015, **2015**, 2794–2803.

24 X. Wang, S. Jin, C. Zhang, L. Li, S. Chen and Q. Shu, *Chin. J. Chem.*, 2015, **33**, 1229–1234.

25 M. Benz, T. M. Klapötke and J. Stierstorfer, *Org. Lett.*, 2022, **24**, 1747–1751.

26 T. M. Klapötke, C. M. Sabaté and J. Stierstorfer, *New J. Chem.*, 2009, **33**, 136–147.

27 J. A. Garrison and R. M. Herbst, *J. Org. Chem.*, 1957, **22**, 278–283.

28 P. Kumar, V. D Ghule and S. Dharavath, *Dalton Trans.*, 2023, **52**, 747–753.

29 M. Jujam, R. Rajak and S. Dharavath, *Adv. Funct. Mater.*, 2025, **35**, 2412638.

30 J. Singh, A. K. Chinnam, R. J. Staples and J. M. Shreeve, *Inorg. Chem.*, 2022, **61**, 16493–16500.

31 S. Li, Y. Wang, C. Qi, X. Zhao, J. Zhang, S. Pang and S. Zhang, *Angew. Chem., Int. Ed.*, 2013, **52**, 14031–14035.

32 J. Zhang, Y. Du, K. Dong, H. Su, S. Zhang, S. Li and S. Pang, *Chem. Mater.*, 2016, **28**, 1472–1480.

33 J. Singh, R. J. Staples and J. M. Shreeve, *J. Mater. Chem. A*, 2025, **13**, 11475–11485.

34 T. M. Klapötke and J. Stierstorfer, *Helv. Chim. Acta*, 2007, **90**, 2132–2150.

35 D. Fischer, T. M. Klapötke and J. Stierstorfer, *Angew. Chem., Int. Ed.*, 2014, **53**, 8172–8175.

36 D. Fischer, T. M. Klapötke and J. Stierstorfer, *Angew. Chem., Int. Ed.*, 2015, **54**, 10299–10302.

37 Y.-N. Li, B.-Z. Wanga, Y.-J. Shu, L.-J. Zhai, S.-Y. Zhang, F.-Q. Bi and Y.-C. Li, *Chin. Chem. Lett.*, 2017, **28**, 117–120.

38 N. Szimhardt, M. H. H. Wurzenberger, P. Spieß, T. M. Klapötke and J. Stierstorfer, *Propellants, Explos., Pyrotech.*, 2018, **43**, 1203–1209.

39 M. Benz, T. M. Klapötke, J. Stierstorfer and M. Voggenreiter, *ACS Appl. Eng. Mater.*, 2023, **1**, 3–6.

40 Q. Yu, P. Yin, J. Zhang, C. He, G. H. Imler, D. A. Parrish and J. M. Shreeve, *J. Am. Chem. Soc.*, 2017, **139**, 8816–8819.

41 J. Singh, R. J. Staples and J. M. Shreeve, *Sci. Adv.*, 2023, **9**, eadk3754.

42 S. G. Zlotin, I. L. Dalinger, N. N. Makhova and V. A. Tartakovsky, *Russ. Chem. Rev.*, 2020, **89**, 1–54.

43 O. T. O'Sullivan and M. J. Zdilla, *Chem. Rev.*, 2020, **120**, 5682–5744.

44 Q. Yu, G. H. Imler, D. A. Parrish and J. M. Shreeve, *Org. Lett.*, 2019, **21**, 4684–4688.

45 V. Thottempudi, H. Gao and J. M. Shreeve, *J. Am. Chem. Soc.*, 2011, **133**, 6464–6471.

46 H. E. Kissinger, *Anal. Chem.*, 1957, **29**, 1702–1706.

47 T. A. Ozawa, *Bull. Chem. Soc. Jpn.*, 2006, **38**, 1881–1886.

48 D. J. Whelan, R. J. Spear and R. W. Read, *Thermochim. Acta*, 1984, **80**, 149–163.

49 Q.-u.-N. Tariq, S. Manzoor, M.-u.-N. Tariq, W.-L. Cao and J.-G. Zhang, *Def. Technol.*, 2022, **18**, 1945–1959.

50 M. A. Ilyushin, I. V. Tselinsky and I. V. Shugalei, *Cent. Eur. J. Energ. Mater.*, 2012, **9**, 293–328.

51 K. Pandey, A. Tiwari, J. Singh, P. Bhatia, P. Das, D. Kumar and J. M. Shreeve, *Org. Lett.*, 2024, **26**, 1952–1958.

17428 | *J. Mater. Chem. A*, 2025, **13**, 17421–17428

This journal is © The Royal Society of Chemistry 2025